Structure, superconducting and magnetotransport properties of $Ru_{1-x}Sn_xSr_2Gd_{1.4}Ce_{0.6}Cu_2O_y$ ($0 \leq x \leq 0.1$)

2008 J. Phys.: Condens. Matter 20 325203

(http://iopscience.iop.org/0953-8984/20/32/325203)

IOP PUBLISHING JOURNAL OF PHYSICS: CONDENSED MATTER
J. Phys.: Condens. Matter **20** (2008) 325203 (8pp) doi:10.1088/0953-8984/20/32/325203

Structure, superconducting and magnetotransport properties of $Ru_{1-x}Sn_xSr_2Gd_{1.4}Ce_{0.6}Cu_2O_y$ $(0 \leqslant x \leqslant 0.1)$

N Balchev[1], K Nenkov[2,3], G Mihova[1], B Kunev[4] and J Pirov[5]

[1] Institute of Solid State Physics, Bulgarian Academy of Sciences, 1784 Sofia, Bulgaria
[2] Institut fur Festkorper- und Werkstofforschung, 01171 Dresden, Germany
[3] International Laboratory of High Magnetic Fields and Low Temperatures, 53-421 Wroclaw, Poland
[4] Institute of Catalysis, Bulgarian Academy of Sciences, 1113 Sofia, Bulgaria
[5] Central Laboratory of Photoprocesses, Bulgarian Academy of Sciences, 1113 Sofia, Bulgaria

Received 14 May 2008, in final form 10 June 2008
Published 9 July 2008
Online at stacks.iop.org/JPhysCM/20/325203

Abstract
Samples with nominal compositions $Ru_{1-x}Sn_xSr_2Gd_{1.4}Ce_{0.6}Cu_2O_y$ $(0 \leqslant x \leqslant 0.1)$ were synthesized and their structure, superconducting and magnetotransport properties were investigated. It was shown that the Sn-doping enhances the crystal growth in Ru-1222. A maximum in the dependences of the lattice parameters and T_c on the dopant content x was observed. Small doping levels significantly increase the T_c of the Ru-1222 samples, prepared at the same conditions—from 20 K for the undoped sample to 35 K for the $x = 0.02$ and 0.03 ones. It was found that the Sn-doping enhances the upper critical field $H_{c2}(0)$, extrapolated to $T = 0$, and the weak link behavior at the expense of the intragranular superconductivity in Ru-1222. The observed phenomena are discussed.

1. Introduction

The discovery of a coexistence of superconductivity (SC) and weak ferromagnetism (FM) in $RuSr_2R_{2-x}Ce_xCu_2O_{10}$ (R = Eu, Gd, Ru-1222) [1] and $RuSr_2GdCu_2O_8$ (Ru-1212) [2] has attracted the attention of the investigators in the last few years. It was established that the magnetism originates from the RuO_2 layers and superconductivity arises from the CuO_2 planes. Therefore the SC and weak FM states are practically decoupled and there is no pair breaking. More information about the SC and magnetic state of Ru-1222 can be obtained if Ru is partially replaced by other ions. The foreign ions can modify the carrier concentration and oxygen content of Ru-1222 and influence its superconducting and magnetic properties. Some reports exist on $(Ru_{1-x}M_x)$-1222 systems where M = Fe, Co, Nb and Mo [3–8]. Sn-substitution has attracted the attention of the investigators since it was established that Sn weakly affects the SC properties of YBaCuO and YBaSrCuO [9]. It was also shown that the Sn-doping favors the melt-texture-growth (MTG) of YBaCuO [10]. The authors of [11, 12] studied the effect of Sn-substitution on the superconducting properties of the Hg-1223 and (Pb, Cu)-1212 systems. It was established that Sn stimulates the Hg-1212 phase formation and enhances both the diamagnetic volume fraction and the weak link behavior. In [13, 14] the substitution of Sn in Ru-1212 was investigated. Superconductivity exists at Sn-concentrations of $x \leqslant 0.5$ for Hg-1223 and $x \leqslant 0.3$ for (Pb, Cu)-1212 and Ru-1212. Luo *et al* [15] synthesized (Cd, Sn)-1222 samples thus showing that Sn can be involved in the phase 1222. The Sn^{4+} ionic radius (0.69 Å) is higher than that of Ru^{4+} (0.62 Å), Ru^{5+} (0.565 Å) and Cu^{2+} (0.65 Å) [16]. This could allow a partial substitution of Sn in the Ru and/or the Cu sites. Felner *et al* [17] studied the magnetization and Mössbauer spectra of Sn-doped Ru-1222. A decrease of T_c and the magnetic transition temperature with an increase of the dopant content was observed. The present work is an investigation of the effect of Sn-doping on the structure, superconducting and magnetotransport properties of Ru-1222. We established a maximum of the lattice parameters and T_c with an increase of the dopant content. It was found that Sn-doping enhances the upper critical field $H_{c2}(0)$ of Ru-1222 and the weak link behavior. The observed phenomena are discussed.

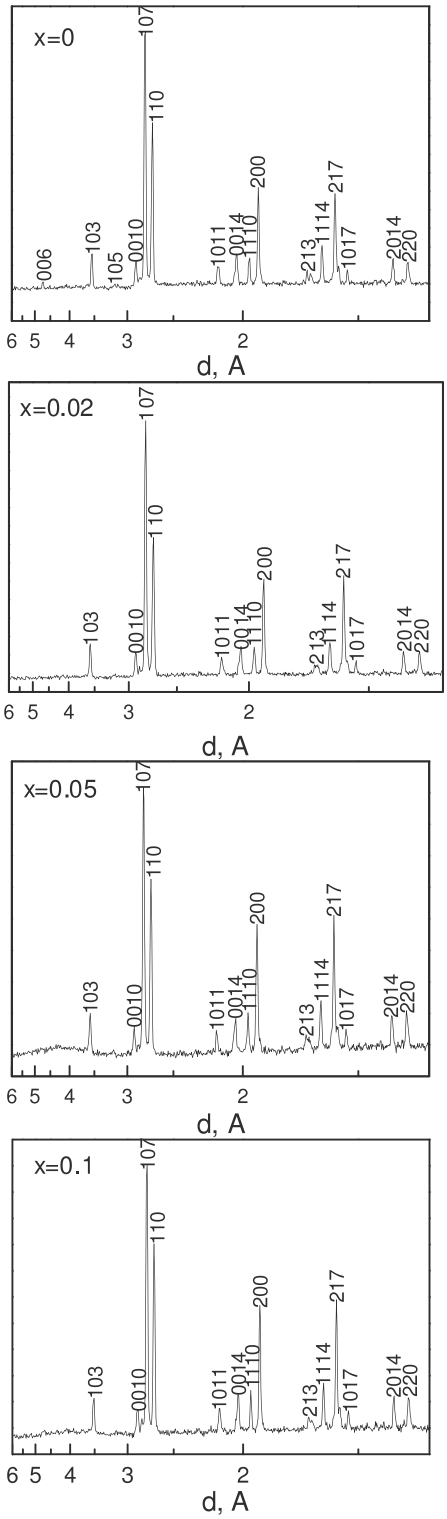

Figure 1. XRD patterns of $Ru_{1-x}Sn_xSr_2Gd_{1.4}Ce_{0.6}Cu_2O_y$ for $x = 0$, 0.02, 0.05 and 0.1.

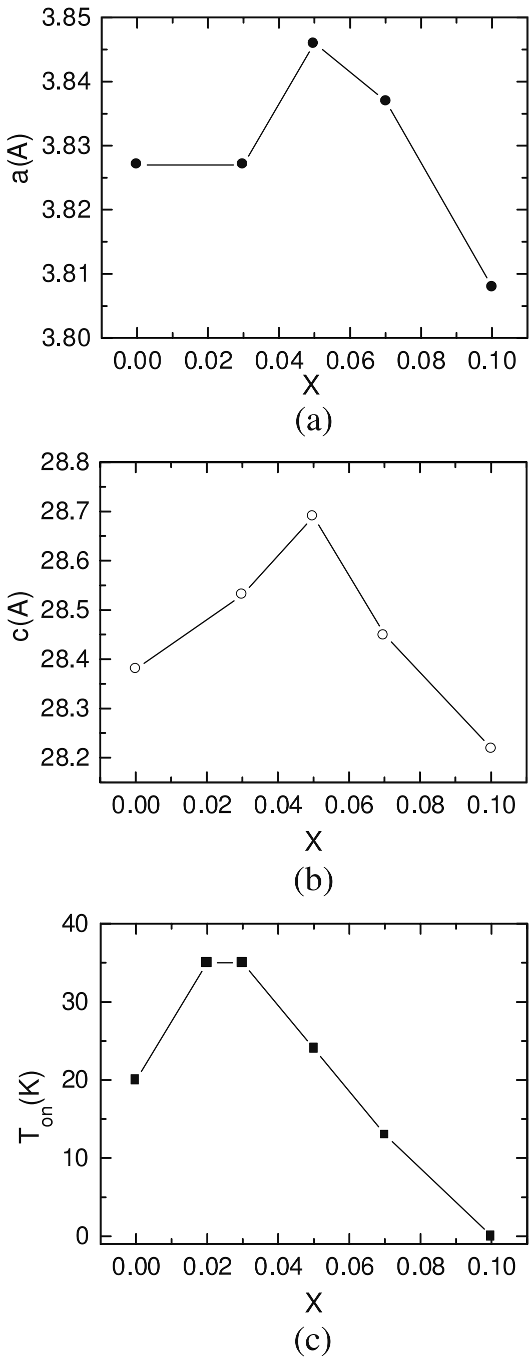

Figure 2. Dependences of the lattice parameters **a**, **c** and T_{on} on x.

2. Experimental results

The investigated samples with nominal compositions $Ru_{1-x}Sn_x$ $Sr_2Gd_{1.4}Ce_{0.6}Cu_2O_y$ ($x = 0$, 0.02, 0.03, 0.05, 0.07 and 0.1) were prepared by a solid state reaction from starting products RuO_2, Gd_2O_3, SnO_2, CeO_2, $SrCO_3$ and CuO with purities above 99.9%. They were mixed, homogenized, pressed into pellets and preheated at 600 °C for 48 h in air and at 1000 °C for 24 h in flowing oxygen. Subsequently they were reground, repressed and sintered at 1060 °C for 96 h in flowing oxygen. Finally they were annealed at 350 °C for 48 h in flowing oxygen. X-ray diffraction (XRD) was used to examine the samples using a TUR-M62 diffractometer and Co Kα radiation. An SEM with EDS analysis was performed on the pellets using an SEM-525 Philips microscope combined with an EDAX 9900 device. The susceptibilities of the samples were measured by a SQUID magnetometer (Quantum Design: PPMS-9T and MPMS-XL7T). The resistivities of the samples ρ versus T were measured by the standard four probe method.

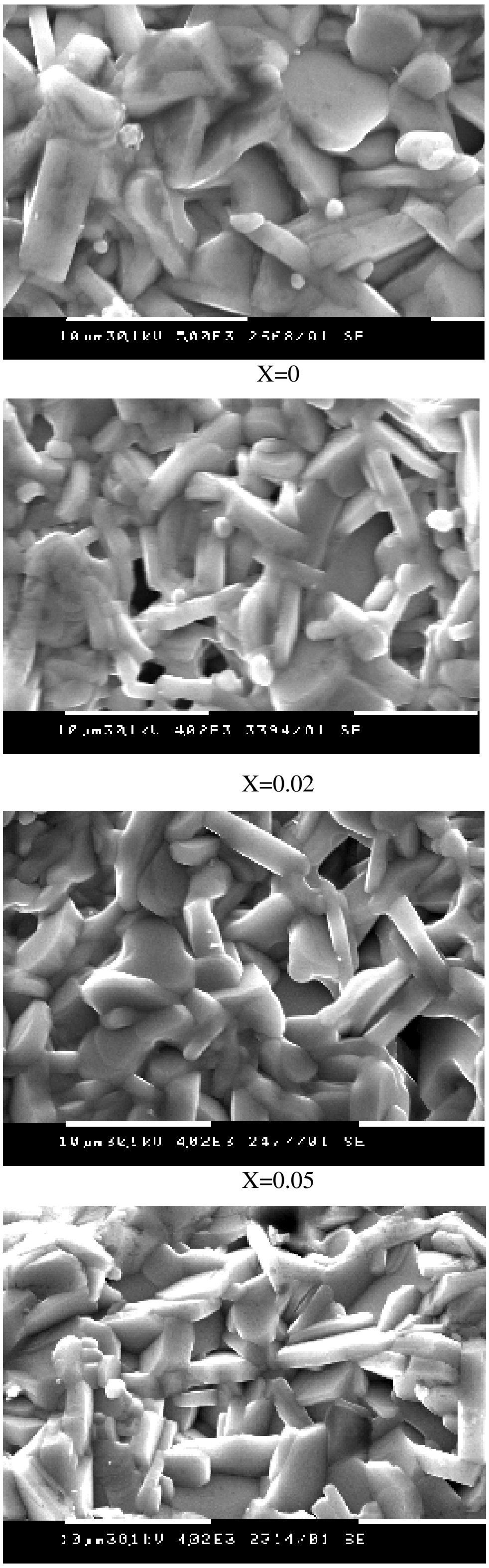

Figure 3. SEM pictures of the $x = 0$, 0.02, 0.05 and 0.1 samples.

Figure 1 shows the XRD patterns of $Ru_{1-x}Sn_xSr_2Gd_{1.4}Ce_{0.6}Cu_2O_y$ for $x = 0$, 0.02, 0.05 and 0.1. It may be seen that the samples are single phased. The dependences of the calculated lattice parameters **a** and **c** on x for all the

Table 1. Distribution of the tin at different points of the $x = 0.02$ sample.

Point	Sn-content (wt%)
1	0.17
2	0.28
3	0.58
4	0.05
5	0
6	0.55

investigated samples are shown in figures 2(a) and (b). It the presence of a maximum may be seen and this will be discussed in section 3. In figure 3 the SEM pictures of the $x = 0$, 0.02, 0.05 and 0.1 samples are given. In the undoped sample several tetragonal microcrystals can be seen but most of the crystal boundaries are not well expressed due to incomplete crystallization. In the doped samples the relative number of tetragonal microcrystals increases. From this we may conclude that the Sn-doping enhances the crystal growth in Ru-1222. The calculated densities of the samples vary from 5.74 g cm^{-3} for $x = 0.02$ to 6.12 g cm^{-3} for $x = 0.07$ and 0.1. For comparison, the authors of [10] obtained densities of 5.66 g cm^{-3} in their Sn-doped MTG YBaCuO samples. Therefore the high densities of the investigated samples may be due to a partial melting during the synthesis. In order to check the Sn-distribution in the doped samples, an EDS analysis was performed at different points of a polished $x = 0.02$ sample (figure 4). The result, given in table 1 shows an inhomogeneous Sn-distribution and an absence of tin at one of the points.

Figure 5(a) shows the resistivity curves of the $x = 0$, 0.05 and 0.07 samples and figure 5(b)—of the $x = 0.02$ and 0.03 samples. The undoped sample has a semiconducting behavior in the normal state and a broad superconducting transition at $T_{on} = 20$ K. A similar dependence was obtained by Escote *et al* [18] in their as-prepared (i.e. not treated under high oxygen pressure) Ru-1222 samples. From this it may be concluded that our pure Ru-1222 sample is underdoped. It should be noted that a T_{on} above 40 K may be obtained for samples synthesized at high oxygen pressure [18–20]. In our case for $x = 0.02$ and 0.03 T_{on} increases significantly—up to 35 K. For the $x = 0.05$ and 0.07 samples T_{on} decreases. The dependence of T_{on} on x for the investigated samples is given in figure 2(c). The increase of T_c correlates with a decrease in the normal state resistivity. A similar phenomenon is observed in Sn-doped Ru-1212 [13] and Mo-doped Ru-1222 [6] but not in Sn-doped Ru-1222 [17]. This may be due to the different regimes of preparation of our samples and those in [17]. The shoulders in the resistive transitions may be explained by granularity effects [20]. It was established that the $x \geqslant 0.1$ samples are not superconducting. This is not observed in other Sn-containing superconducting systems, where SC exists up to $x \leqslant 0.3$ [9, 11–14]. Therefore the Sn-doping more rapidly destroys the SC in Ru-1222 than in conventional superconductors. A similar phenomenon is observed in Fe-doped Ru-1222 [3] and Co-doped Ru-1222 [7] and this will be discussed in section 3.

In figure 6 we show the $\rho(T)$ curves of the $x = 0.02$ sample at $H = 0$ (inset), 0.05, 0.5, 1, 7 and 9 T. They are

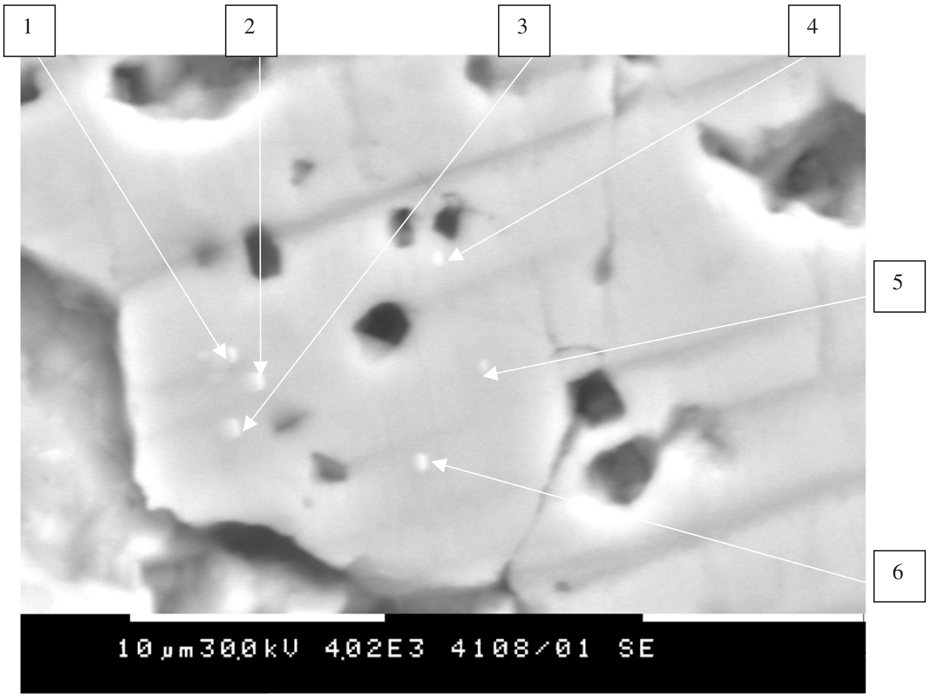

Figure 4. SEM picture of a polished surface of the $x = 0.02$ sample with marked points used for EDS analysis.

similar to those of undoped Gd-containing Ru-1222 samples annealed at high oxygen pressure [18, 20]. With an increase of the magnetic field, the SC transition becomes broader near the onset and sharper near the zero resistance state, which is a characteristic feature of granular superconductors. Also T_{on} decreases slightly from 35 K at $H = 0$ to about 30 K at $H = 9$ T and the zero resistance is preserved above 2 K at this high magnetic field. The curves indicate a high second critical field in the Sn-doped samples. In order to determine this parameter, the H_{c2} versus T phase diagram is given in figure 7. The (H_{c2}, T) pairs are obtained from the 50% drops in the resistivities at different fields. The line corresponds to a fit to the exponential decay of second order $H_{c2}(T) = H_{cJ}\exp(-T/T_1) - H_{cI}\exp(-T/T_2)$ and yields $H_{cJ} \sim 38$ T, $H_{cI} \sim 0.42$ T, $T_1 = 4.24$ K and $T_2 = -4.97$ K. On the other hand, we obtain a value of $\mathrm{d}H_{c2}/\mathrm{d}T = -2.03$ T K^{-1} at $T = 6$ K from the derivative, shown in the inset. By using the Werthamer, Helfand and Hohenberg (WHH) formula $H_{c2}(0) = -0.7(\mathrm{d}H_{c2}/\mathrm{d}T)T_c$ [21], the orbital critical field extrapolated to $T = 0$ can be calculated. Taking $\mathrm{d}H_{c2}/\mathrm{d}T = -2.03$ and $T_c = 30$ K we obtain $H_{c2}(0) \sim 42$ T. At $T = T_{cI} = 25$ K (see figure 9) $\mathrm{d}H_{c2}/\mathrm{d}T = -0.02$ and the WHH formula gives $H_{c2} \sim 0.42$ T. The values calculated by the WHH formula for H_{c2} are in general agreement with those obtained by the fitting curve constants H_{cJ} and H_{cI}. Therefore the latter could be related to the intergrain and intragrain critical fields of Sn-doped Ru-1222 respectively. The value of $H_{c2}(0) \sim 42$ T is higher than that of Escote *et al* [18] for undoped Gd-containing Ru-1222 samples in the WHH approximation—about 31 T. However, according to [18], in pure Ru-1222 H_{c2} remains at about 8 T near T_c. From this we may conclude that the optimum Sn-doping enhances the upper critical field $H_{c2}(0)$, extrapolated to $T = 0$, of Ru-1222 but decreases the intragrain critical field.

Figure 8 shows the $\mathrm{d}\rho/\mathrm{d}T$ versus T dependences for the $x = 0$ sample at $H = 0$ and the $x = 0.02$ sample—at $H = 0$ at 0.05 T. According to [20] the two peaks of the pure sample (figure 8(a)) denote the intragranular and intergranular SC transitions. The derivative of the $x = 0.02$ sample (figure 8(b)) shows a single peak at $H = 0$. However, even at the lowest applied field of 0.05 T one can see both the peaks. This is not observed in pure Ru-1222, where a single peak exists over a wide field range [22]. The result obtained confirms the presence of a low intragrain critical field in the Sn-doped Ru-1222.

In figure 9 the $\chi'(T)$ dependences of ZFC $x = 0$ and 0.03 samples at $H = 0$ are given. It may be seen that negative values of χ' are observed for the $x = 0.03$ sample. The lack of negative values of χ' for $x = 0$ is often observed in Ru-1222 and could be explained by the presence of a spontaneous vortex phase [23]. Also the intragrain and intergrain critical temperatures T_{cI} and T_{cJ} are observed in the curve of the $x = 0.03$ sample.

3. Discussion

First we will discuss the maximum in the dependences of the lattice parameters with the increase of the dopant content. The initial increase of these parameters with x is probably due to the higher ionic radius of Sn^{4+} in comparison with that of Ru^{4+} and Ru^{5+}. The decrease of the lattice parameters at higher doping levels may be associated with a possible distortion and tilt of the RuO_6 octahedra because the Sn ions have distorted

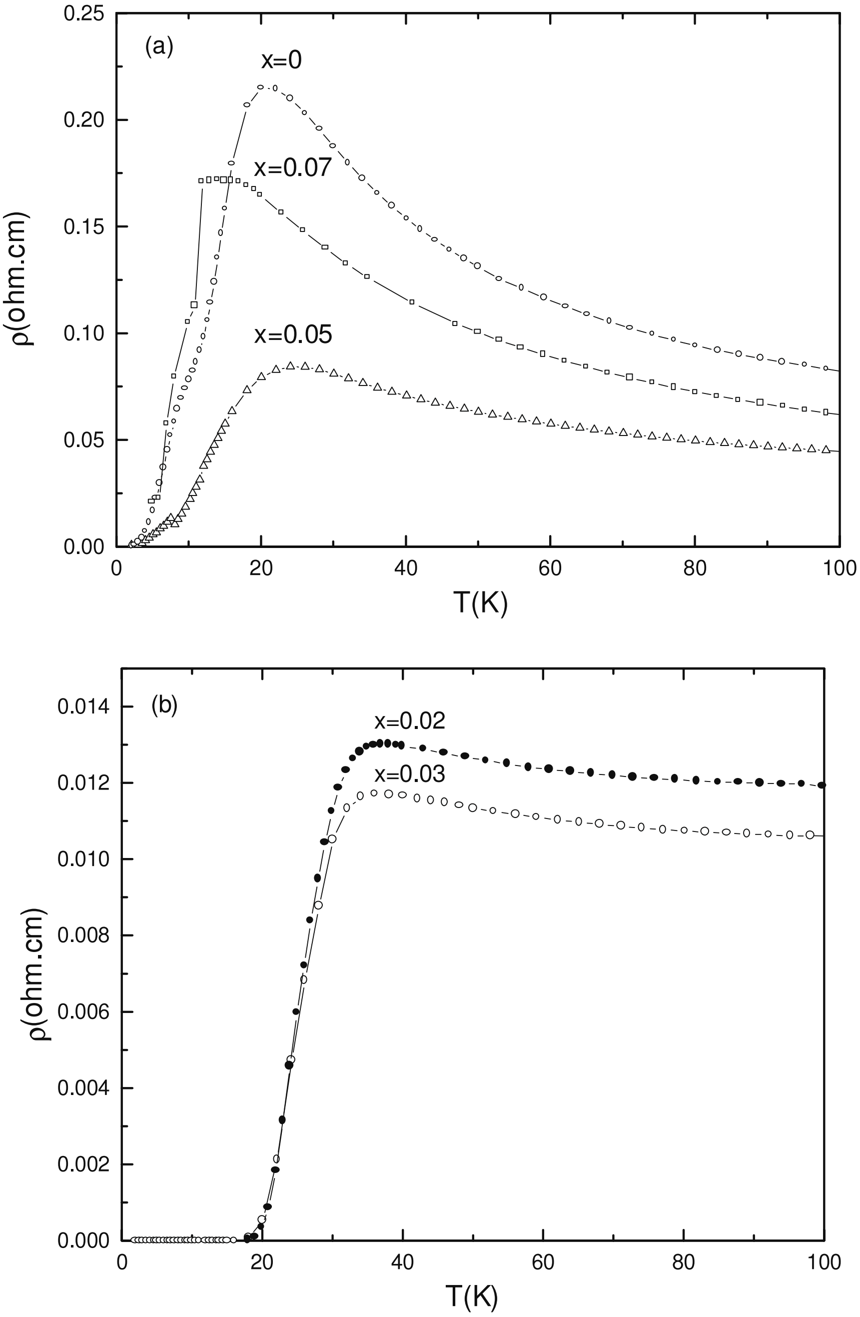

Figure 5. $\rho(T)$ dependences of $Ru_{1-x}Sn_xSr_2Gd_{1.4}Ce_{0.6}Cu_2O_y$ for (a) $x = 0$, 0.05 and 0.07 and (b) $x = 0.02$ and 0.03.

environments when replacing the Ru ions in Ru-1222 [17]. The latter effect will also affect the magnetic state in the Sn-doped Ru-1222 because the weak FM originates from canting of the Ru moments, which depends on the tilting of the RuO_6 octahedra [24]. The magnetic state in the Sn-doped Ru-1222 is investigated in our previous work [25].

In order to explain the presence of a maximum in the dependence of T_c on x, we may assume that the Ru ions are pentavalent (or in a mixed Ru^{4+}/Ru^{5+} state) in the undoped Ru-1222. Since the Sn ions are tetravalent, we may suppose that, with the increase of the doping level the hole concentration p increases. The presence of a maximum in the dependence of T_c on x correlates with the established universal dependence of T_c on the hole concentration p—an initial increase, the presence of a plateau or a broad maximum and then a decrease [26]. Since the carrier concentration and oxygen content are mutually related, an increase of the oxygen content at low doping levels would optimize the T_c of the investigated samples. The decrease of T_c and the rapid suppression of SC at higher doping levels may be explained if we suppose that Sn resides at both Ru and Cu sites. In this case Sn would modify the hole concentration and would create a disorder in the CuO_2 planes [7]. A decrease of the oxygen content at higher doping levels, related to a disorder would strongly affect the resistivity and occurrence of superconductivity in Ru-1222 [27].

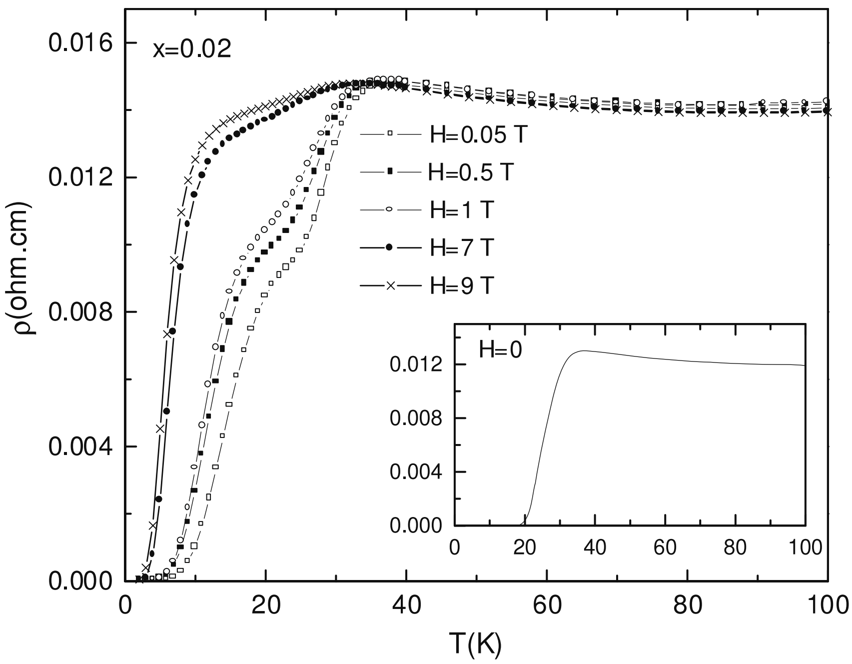

Figure 6. $\rho(T)$ dependences of the $x = 0.02$ sample at $H = 0$ (inset), 0.05, 0.5, 1, 7 and 9 T.

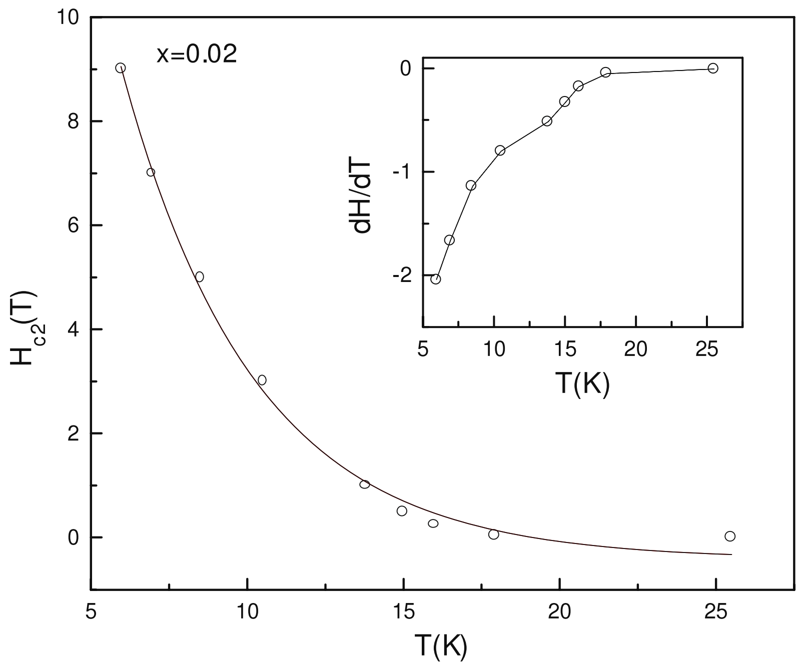

Figure 7. Temperature dependence of the upper critical field H_{c2} of the $x = 0.02$ sample. Inset: dependence of dH_{c2}/dT on T.

In order to discuss the behavior of H_{c2} around $T = 0$ and T_c, we emphasized that the SC properties of the investigated samples are influenced by granular effects. The granular superconductivity is expressed by the presence of a two step resistive transition and lack of diamagnetism between the intragrain (T_{cI}) and intergrain (T_{cJ}) critical temperatures [28]. The constants H_{cJ} and H_{cI} obtained from the fitting curve and those of H_{c2} calculated by the WHH formalism suggest that Sn-doping enhances the intergrain, but decreases the intragrain critical field of Ru-1222. This means that the Sn-doping enhances the weak link behavior of the undoped system. The obtained SEM images, shown in figure 3 and the high densities of the samples point towards a strong intergrain coupling, as in the case of the pure Eu-containing Ru-1222, synthesized at 1090 °C [22]. A weak link behavior may arise from Josephson junctions between regions with different oxygen content, as suggested in [20]. The inhomogeneous tin distribution, illustrated in table 1 suggests the presence of

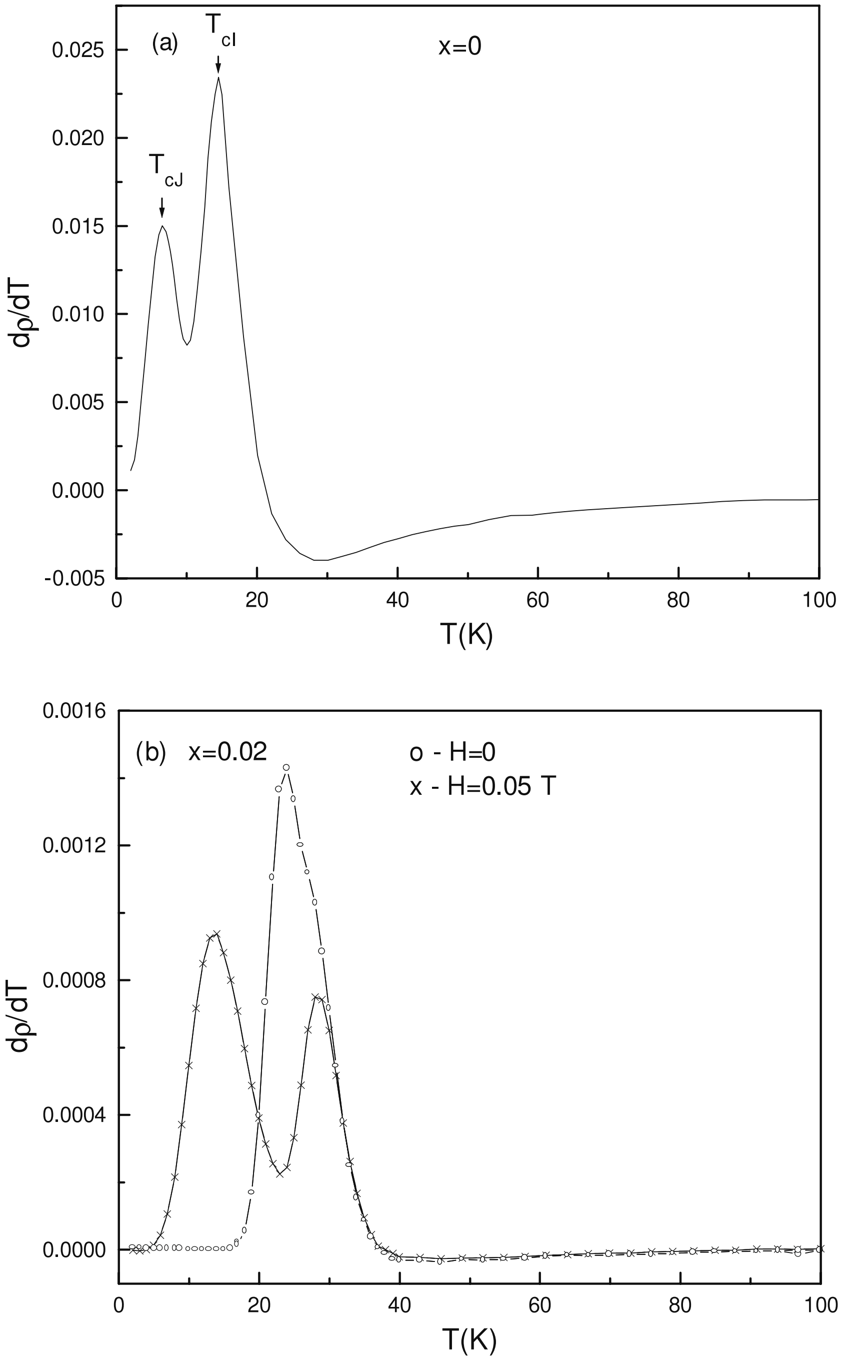

Figure 8. $d\rho/dT$ versus T dependence of: (a) the $x = 0$ sample at $H = 0$ and (b) the $x = 0.02$ sample at $H = 0$ and 0.05 T.

a Josephson array of regions with different Sn (respectively oxygen) content in the microcrystals. In this case the weak link behavior would be enhanced at the expense of the intragrain superconductivity.

4. Conclusion

In conclusion, we synthesized samples with nominal compositions $Ru_{1-x}Sn_xSr_2Gd_{1.4}Ce_{0.6}Cu_2O_y$ ($0 \leqslant x \leqslant 0.1$) and investigated their structure, superconducting and magnetotransport properties. It was shown that Sn-doping enhances the crystal growth in Ru-1222. A maximum in the dependences of the lattice parameters and T_c on the dopant content x was observed. It was established that small doping levels ($x = 0.02$ and 0.03) significantly increase the T_c of the Ru-1222 samples, prepared at the same conditions—from 20 K for the undoped sample to 35 K for the $x = 0.02$ and 0.03 ones. The initial increase of T_c was associated with an increase of the hole concentration. The decrease of T_c and the suppression of SC at higher doping levels may be explained by an enhanced disorder in the system, due to the possible presence of Sn at both Ru and Cu sites. It was found that Sn-doping enhances

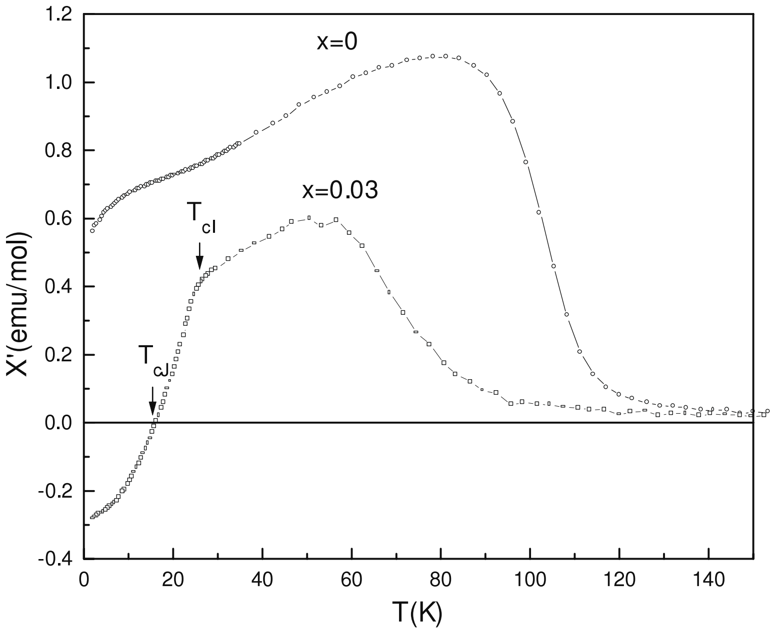

Figure 9. Temperature dependence of χ' at $H = 0$ for ZFC $x = 0$ and 0.03 samples.

the upper critical field $H_{c2}(0)$, extrapolated to $T = 0$, and the weak link behavior at the expense of the intragranular superconductivity in Ru-1222. The observed phenomena were discussed.

Acknowledgments

This research is financially supported by the Institute of Solid State Physics (Grant No BK-2). The authors gratefully acknowledge Dr V Rusanov from the Department of Physics, University of Sofia for helpful discussions.

References

[1] Felner I, Asaf U, Levi Y and Millo O 1997 *Phys. Rev.* B **55** R3374

[2] Bernhard C, Tallon J L, Niedermayer Ch, Blasius Th, Golnik A, Brucher E, Kremer R K, Noakes D R, Stronach C E and Ansaldo E J 1999 *Phys. Rev.* B **59** 14099

[3] Felner I and Asaf U 1997 *Physica* C **292** 97

[4] Kuzmicheva G M, Andreenko A S, Kostyleva I E, Zalevski A and Warchulska J 2003 *Physica* C **400** 7

[5] Lee H K and Williams G V M 2004 *Physica* C **415** 172

[6] Awana V P S, Lal R, Kishan H, Narlikar A V, Peurla M and Laiho R 2006 *Phys. Rev.* B **73** 014517

[7] Awana V P S, Kishan H, Eshkenazi O, Felner I, Rawat R, Ganesan V and Narlikar A V 2007 *J. Phys.: Condens. Matter* **19** 026203

[8] Cardoso C A, Araujo-Moreira F M, Awana V P S, Kishan H and de Lima O F 2007 *J. Phys.: Condens. Matter* **19** 186225

[9] Zhao Y, Chen B, Kennedy H, Zhang H and Wang F 1995 *Physica* C **252** 381

[10] Fung P C W, Du Z L, Chow J C L, He Z H, Yu T F, Luo Y Y, Li Q Y and Lu Y 1993 *Physica* C **212** 279

[11] Balchev N, Van Allemeersch F, Persyn F, Schroeder J, Deltour R and Hoste S 1997 *Supercond. Sci. Technol.* **10** 65

[12] Balchev N, Nenkov K, Kunev B, Souleva A, Tsacheva T S and Hoste S 2001 *J. Supercond. Novel Magn.* **14** 711

[13] McLaughlin A C and Attfield J P 1999 *Phys. Rev.* B **60** 14605

[14] Williams G V M, Lee H K and Kramer S 2003 *Phys. Rev.* B **67** 104514

[15] Luo H, Chen Z, Qian Y T, Shi I and Zhou G 1997 *J. Alloys Compounds* **257** 46

[16] Shannon R D 1976 *Acta Crystallogr.* A **32** 751

[17] Felner I, Galstyan E, Herber R H and Nowik I 2004 *Phys. Rev.* B **70** 094504

[18] Escote M T, Meza V A, Jardim R F, Ben-Dor L, Torikachvili M S and Lacerda A H 2002 *Phys. Rev.* B **66** 144503

[19] Chen X H, Sun Z, Wang K Q, Li S Y, Xiong Y M, Yu M and Cao L Z 2001 *Phys. Rev.* B **63** 064506

[20] Krasovitsky V B, Belevtsev B I, Beliayev E Yu, Naugle D G, Rathnayaka K D D and Felner I 2006 *J. Phys: Conf. Ser.* **51** 283

[21] Tinkham M 1975 *Introduction to Superconductivity* (New York: McGraw-Hill)

[22] Nigam R, Pan A V and Dou S X 2007 *J. Appl. Phys.* **101** 09G109

[23] Sonin E B and Felner I 1998 *Phys. Rev.* B **57** R14000

[24] Zivkovic I, Hirai Y, Frazer B H, Prester M, Drobac D, Ariosa D, Berger H, Pavuna D, Margaritondo G, Felner I and Onellion M 2002 *Phys. Rev.* B **65** 144420

[25] Balchev N, Nenkov K, Mihova G, Kunev B and Pirov J 2007 *Physica* C **467** 174

[26] Zhang H and Sato H 1993 *Phys. Rev. Lett.* **70** 1697

[27] Cardoso C A, Lanfredi A J C, Chiquito A J, Araujo-Moreira F M, Awana V P S, Kishan H, de Almeida R L and de Lima O F 2005 *Phys. Rev.* B **71** 134509

[28] Jardim R F, Ben-Dor L, Stroud D and Maple M B 1994 *Phys. Rev.* B **50** 10080